

Structural and Optical Properties of Samarium Doped Sr<sub>2</sub>CeO<sub>4</sub> via Solid State Reaction Method.Pradip Z Zambare<sup>1\*</sup>, and OH Mahajan<sup>2</sup><sup>1</sup>Department of Physics, SVS's Dadasaheb Rawal College, Dondaicha, Maharashtra 425408, India.<sup>2</sup>Department of Physics, MJ College Jalgaon, Maharashtra, India.

## Research Article

Received: 11/06/2013

Revised: 17/06/2013

Accepted: 23/06/2013

**\*For Correspondence**Department of Physics, SVS's  
Dadasaheb Rawal College, Dondaicha,  
Maharashtra 425408, India.**Keywords:** Photoluminescence, solid  
state reaction method, Sr<sub>2</sub>CeO<sub>4</sub>, XRD,  
phosphor.**ABSTRACT**

Strontium cerium oxide Sr<sub>2</sub>CeO<sub>4</sub> doped Sm<sup>3+</sup> phosphor was synthesized by solid state reaction method at temperature 1200° C for 4h. The powder samples were characterized by X-ray diffraction (XRD), Raman spectra, Fourier Transform infrared spectra (FTIR), Scanning Electron microscope (ESM), Energy dispersive spectra (EDS), and photoluminescence. The X-Ray diffraction pattern reveals the crystallite size and the structure is orthorhombic. Photoluminescence excitation and emission spectra of Sr<sub>2</sub>Ce O<sub>4</sub>: xSm<sup>3+</sup> (0.5 ≤ x ≤ 1.5) are recorded at room temperature. The color co-ordinates for the Sr<sub>2</sub>Ce O<sub>4</sub>: 1.0 mol % Sm<sup>3+</sup> were x = 0.6687 and y = 0.3311. This phosphor has a good potential for applications in display devices.

**INTRODUCTION**

The Rare earth materials have attracted much attention for their impressive applications in artificial light, X-ray medical radiography, lamps and display devices [1, 2]. The discovery and development of new phosphor materials is of great importance for the advance of flat panel display and illumination technology. Compared with organic materials and sulfide phosphors, oxide-based phosphors have the advantage: stable crystalline structure and high physical and chemical stability. Therefore, oxide-based phosphors, especially rare earth-based oxide phosphor are attracting more and more attention [3,4,5]. It has been found that the luminescence materials with low-dimensional structures generally exhibit special luminescence properties [6, 7]. Sr<sub>2</sub>CeO<sub>4</sub> consists of infinite edge-sharing CeO<sub>6</sub> octahedra chains separated by Sr atoms. Luminescence originates from a ligand to metal Ce<sup>4+</sup> charge transfer. The broad emission band of Sr<sub>2</sub>CeO<sub>4</sub> blue phosphor 471 nm is suitable for the doping of rare earth ions in pursuing new luminescent materials. The rare earth materials exhibit excellent sharp-emission luminescence properties with suitable sensitization and effectively used in designing of white light emitting materials [6,7,8,9]. In this paper, the formation process, micro-structure and luminescent properties of the synthesized Sr<sub>2</sub>CeO<sub>4</sub>: xSm<sup>3+</sup> (0.5 ≤ x ≤ 1.5) were investigated.

**MATERIALS AND METHODS**

The starting materials were Strontium Carbonate SrCO<sub>3</sub>, Cerium Oxide CeO<sub>2</sub>, and Samarium Oxide Sm<sub>2</sub>O<sub>3</sub> of 99.9 % purity. These materials were taken in Stoichiometric proportions of Sr: Ce as 2:1. SrCO<sub>3</sub> and CeO<sub>2</sub> with rare earth were weighed in molecular stoichiometry. These all materials were ground in an agate mortar and pestle, grinded thoroughly to get fine powder. This powder was taken in alumina crucible. After closing the cover, the crucible was loaded in furnace and heated to the temperature 1200 °C at the rate 300 °C/hr. The samples were kept at the set temperature for four hours then cooled down naturally. All samples were prepared by same technique.

The structural studies were carried out by X-ray diffraction technique in reflection mode with filtered Cu Kα radiation (λ = 1.54051 Å) with Rigaku, D Max III VC, Japan. Raman spectra were recorded on Renishaw Invia Raman microscope. The FTIR spectrums were recorded on SHIMADZU IR Affinity-1 model transmission spectrometer with KBr pellet method over the range 400–4000 cm<sup>-1</sup>. The photoluminescence spectra was recorded at room temperature using Spectrofluorophotometer (SHIMADZU, RF – 5301 PC) using Xenon lamp as excitation source.

RESULTS AND DISCUSSION

The typical X-ray diffraction pattern of the resultant  $\text{Sr}_2\text{CeO}_4:\text{xSm}^{3+}$  ( $0.5 \leq \text{x} \leq 1.5$ ) phosphors prepared via the solid state reaction method are shown in fig. 1. The patterns of the samples ( $0.5 \leq \text{x} \leq 1.5$ ) were well consistent with the data indicated in JCPDS card No. 50-0115 [2] and structure of  $\text{Sr}_2\text{CeO}_4$  phosphor is orthorhombic. The calculated average crystallite size of the  $\text{Sr}_2\text{CeO}_4$  phosphor is 22 nm [7]. When Samarium doped with  $\text{Sr}_2\text{CeO}_4$  the crystallite size is increases which is shown in table1.

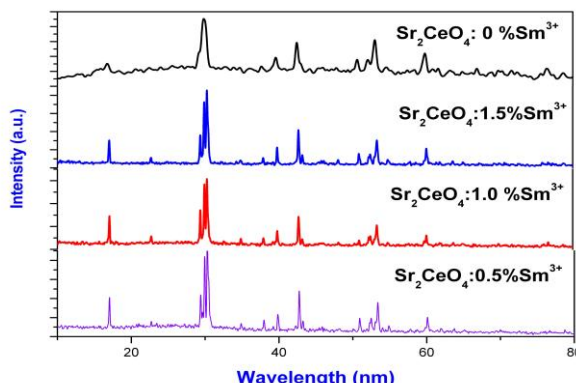


Figure 1: XRD Pattern of  $\text{Sr}_2\text{CeO}_4:\text{Sm}^{3+}$

Phosphors	Crystallite size
$\text{Sr}_2\text{CeO}_4: 0\% \text{Sm}^{3+}$	22nm
$\text{Sr}_2\text{CeO}_4: 0.5\% \text{Sm}^{3+}$	35 nm
$\text{Sr}_2\text{CeO}_4: 1.0\% \text{Sm}^{3+}$	46 nm
$\text{Sr}_2\text{CeO}_4: 1.5\% \text{Sm}^{3+}$	50 nm

Table 1: Showing Crystallite size for different concentration

As doping concentration increases from 0 to 1.5 %, the crystallinity of  $\text{Sr}_2\text{CeO}_4:\text{xSm}^{3+}$  ( $0.5 \leq \text{x} \leq 1.5$ ) phosphor was decrease slightly with the increase in doping amount of  $\text{Sm}^{3+}$ . Samarium ions were doped to substitute strontium ions in the host lattice of  $\text{Sr}_2\text{CeO}_4$  due to the similar ionic radius and electric charge. However the difference of ionic radius of  $\text{Sr}^{2+}$  (For 6-coordination, ionic radius of  $\text{Sm}^{3+}$  (0.0958 nm) was smaller than that of  $\text{Sr}^{2+}$  (0.118 nm), would lead to destroy the crystal structure of  $\text{Sr}_2\text{CeO}_4$ , resulting in the formation of  $\text{SrCeO}_3$  and decrease in crystallinity of  $\text{Sr}_2\text{CeO}_4$ .

In order to study the morphology of the  $\text{Sr}_2\text{CeO}_4:\text{Sm}^{3+}$ , SEM analysis was carried out. Figure 2 a) shows the SEM photograph of  $\text{Sr}_2\text{CeO}_4:\text{Sm}^{3+}$  powder prepared via the solid state reaction method heating at 1200 °C for 4h. From the results it is clear that the particles of  $\text{Sr}_2\text{CeO}_4: 1 \text{ mol } \% \text{Sm}^{3+}$  is in irregular shape and loosely agglomerated. EDS was performed to further confirm the composition of the obtained products. Figure 2 b) indicates that the product is composed of Sr, Ce, O, and Sm with an approximate molar ratio of 1.99:1:4:0.01, which is in good agreement with those of the feed.

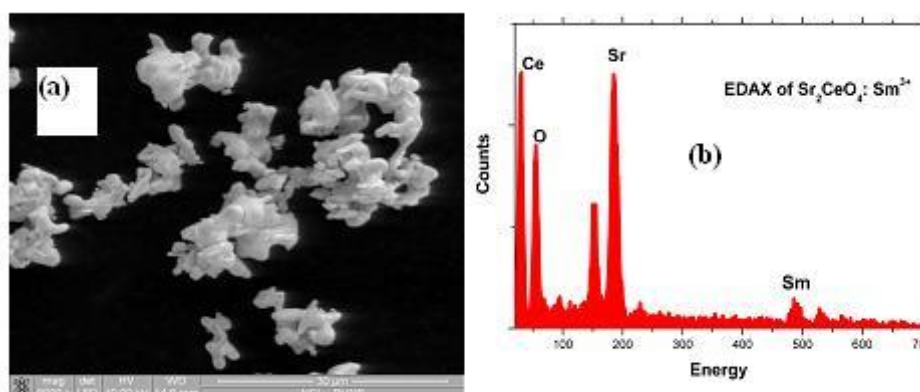


Figure 2: a) SEM of  $\text{Sr}_2\text{CeO}_4:\text{Sm}^{3+}$  and b) EDS of  $\text{Sr}_2\text{CeO}_4:\text{Sm}^{3+}$

The synthesized  $\text{Sr}_2\text{CeO}_4:\text{x mol } \% \text{Sm}^{3+}$  ( $0.5 \leq \text{x} \leq 1.5$ ) prepared by solid state reaction method has been subjected to Fourier transform infrared studies, which are used to analyze qualitatively the presence of functional group in the powder. The FTIR spectrums of powders were recorded using IR affinity-1 made by Shimadzu FTIR Spectrometer by KBr pellet technique. The FTIR spectrum of the  $\text{Sr}_2\text{CeO}_4$  is shown in Fig. 3. The peaks at  $2316 \text{ cm}^{-1}$  are assigned to water molecules that may be present due to

absorption of moisture. usually present in KBr respectively. The absorption peaks at 1444, 1072, and 486  $\text{cm}^{-1}$  were assigned to stretching characteristics of  $\text{SrCO}_3$  [4].

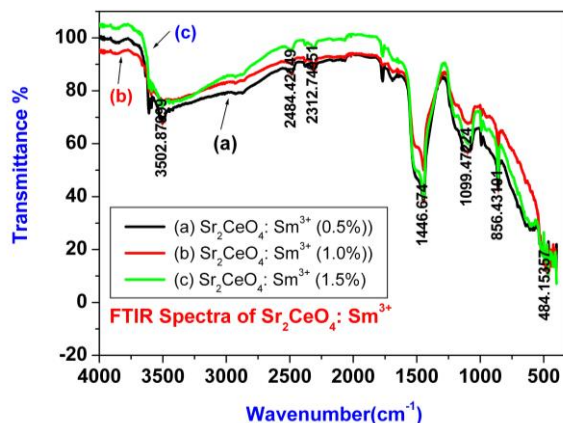


Figure 3: FTIR spectra of  $\text{Sr}_2\text{CeO}_4: \text{Sm}^{3+}$

Raman spectroscopy is very useful tool to determine the phase and structure of multioxide system [6]. The figure 4 shows room temperature Raman spectra of  $\text{Sr}_2\text{CeO}_4: x \text{ mol } \% \text{Sm}^{3+}$  ( $0.5 \leq x \leq 1.5$ ) sample calcinated at 1200  $^\circ\text{C}$  temperature for 4h. The Raman band at 557  $\text{cm}^{-1}$  is assigned to symmetric stretching mode of  $\text{SrCO}_3$  which coincide well with the IR features. The band at 553  $\text{cm}^{-1}$  is attributed to antisymmetric bending vibration. Two strong Raman bands at 286 and 385  $\text{cm}^{-1}$  are detected, which can be attributed to the stretching modes of the  $\text{Ce}-\text{O}_2$  and  $\text{Ce}-\text{O}_1$  of  $\text{CeO}_6$  octahedra in  $\text{Sr}_2\text{CeO}_4$  respectively. So the contribution of  $\text{Ce}-\text{O}_2$  bonds increases corresponding with  $\text{Ce}-\text{O}_1$  bonds to induce the charge transfer [5], which related to the luminescence of this material.

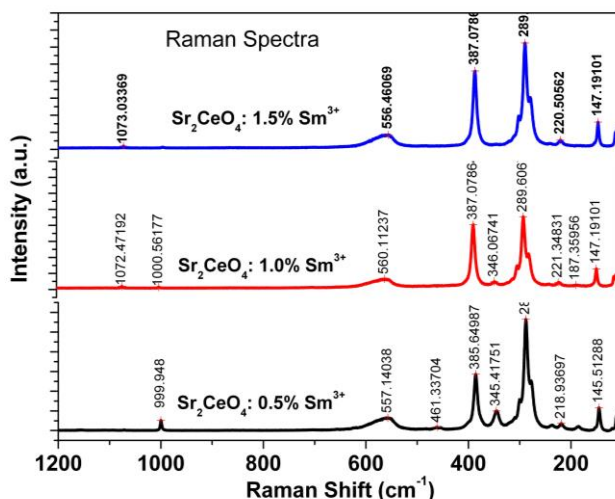


Figure 4: Raman Spectrum of  $\text{Sr}_2\text{CeO}_4: \text{Sm}^{3+}$

### Luminescent Properties

The excitation spectra of solid state reaction derived  $\text{Sr}_2\text{CeO}_4: x\text{Sm}^{3+}$  ( $0.5 \leq x \leq 1.5$ ) calcinated at 1200  $^\circ\text{C}$  for 4h, as shown in figure 5. The excitation spectra is broad spectra from 220 to 400 nm and centered located at 356 nm. The broad band could be assigned to the ligand to-metal charge transfer from  $\text{O}^{2-}$  to  $\text{Ce}^{4+}$ .

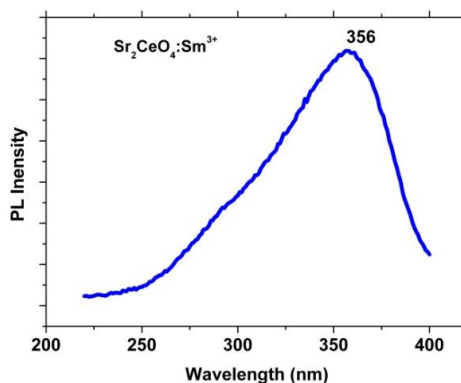


Figure 5: Excitation spectra of  $\text{Sr}_2\text{CeO}_4: \text{Sm}^{3+}$

The emission bands in figure 6 can be attributed into two groups corresponding to different transition of  $\text{Sm}^{3+}$  [6]. The emission peak at 568 nm corresponds to  ${}^4\text{G}_{5/2} \rightarrow {}^6\text{H}_{5/2}$  transition, 611 nm corresponds to  ${}^4\text{G}_{5/2} \rightarrow {}^6\text{H}_{7/2}$  transition and the transition 653 nm corresponds to  ${}^4\text{G}_{5/2} \rightarrow {}^6\text{H}_{9/2}$ , the strongest emission peak located at 611 nm showing prominent and red light is due to the  ${}^4\text{G}_{5/2} \rightarrow {}^6\text{H}_{7/2}$  magnetic dipole transition of  $\text{Sm}^{3+}$ .

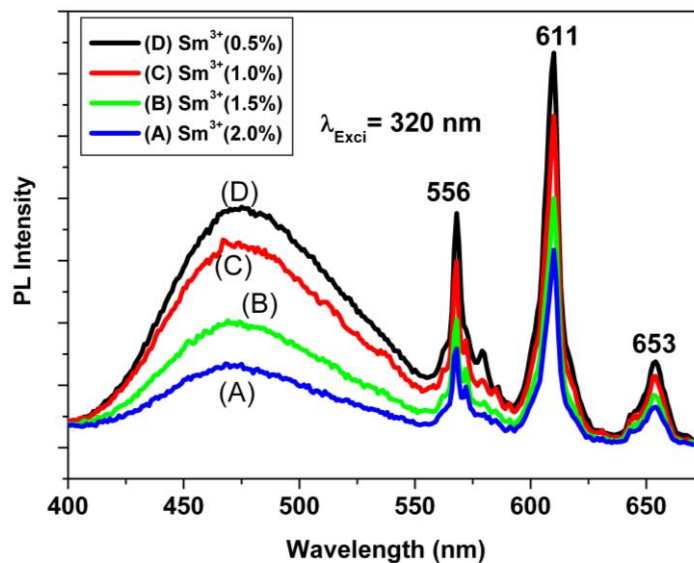


Figure 6: Emission spectra of  $\text{Sr}_2\text{CeO}_4: \text{Sm}^{3+}$

To study the effect of trivalent samarium doping and to see the effect of the same on the emission characteristics of the host, photoluminescence spectra were recorded at room temperature for the  $\text{Sr}_2\text{CeO}_4: x\text{Sm}^{3+}$  ( $x = 0.5\%$ ,  $1\%$ ,  $1.5\%$ ) as shown in figure 2. Under excitation with 320 nm wavelength the emission spectra shows the broad  $\text{Ce}^{4+}-\text{O}^{2-}$  charge transfer band in the blue region superimposed with the  $\text{Sm}^{3+}$  emission lines in the yellow and red region. These spectral features are characteristic of intra-configurationally f-f transitions of the RE ions. Because tetravalent cerium in  $\text{Sr}_2\text{CeO}_4$  has no 4f electrons, emissions are due to the presence of  $\text{Sm}^{3+}$  having five 4f electrons. But on increasing the samarium concentration the sharp lines of the samarium emission appear prominently and the  $\text{Ce}^{4+}-\text{O}^{2-}$  CT transitions of the host decreases relatively. The narrow lines are assigned to the transitions from the between  ${}^4\text{G}_{5/2}$  excited state to the lower  ${}^6\text{H}_j$  ( $j = 5/2, 7/2$  and  $9/2$ ) energy levels of the ground multiplets of  $\text{Sm}^{3+}$ . According to the selection rules [15] magnetic dipole transitions that obey  $J = 0$  and  $\pm 1$  ( $J = \text{total angular momentum}$ ) are allowed for  $\text{Sm}^{3+}$  in a site with inversion symmetry. The emission spectra for the  $\text{Sr}_2\text{CeO}_4$  sample were peaking at the 469 nm but when doped with samarium, the emission spectra are dominated by the red  ${}^4\text{G}_{5/2} \rightarrow {}^6\text{H}_{7/2}$  transition centered at 611 nm. Additional emission were observed at the 568 and 653 nm ascribed to the  ${}^4\text{G}_{5/2} \rightarrow {}^6\text{H}_{5/2}$  and  ${}^4\text{G}_{5/2} \rightarrow {}^6\text{H}_{9/2}$  transitions, respectively.

The emission spectra shows broad  $\text{Ce}^{4+}-\text{O}^{2-}$  CT emission band in the blue-green region superimposed with the  $\text{Sm}^{3+}$  emission lines in the yellow and orange-red regions. It is further observed from the emission spectra of  $\text{Sr}_2\text{CeO}_4: x\text{Sm}$  (0.5 to 2%), that as the samarium concentration increases, the photoluminescence intensity at 468 nm goes on decreasing but the intensity at 568 nm and 611 nm shows an increase for Samarium (0.5 mol%) concentrations.

### CIE Co-ordinates

Most lighting specifications refer to colour in terms of the 1931 CIE chromatic colour coordinates which recognize that the human visual system uses three primary colours: red, green, and blue. The dominant wavelength is the single monochromatic wavelength that appears to have the same colour as the light source. The dominant wavelength can be determined by drawing a straight line from one of the CIE white illuminants ( $C_s$  (0.3101, 0.3162)), through the ( $x, y$ ) coordinates to be measured, until the line intersects the outer locus of points along the spectral edge of the 1931 CIE chromatic diagram [12,13,14].

The colour co-ordinates for the pure  $\text{Sr}_2\text{CeO}_4$  were  $x = 0.1515$  and  $y = 0.1674$  and  $\text{Sm}$ , doped  $\text{Sr}_2\text{CeO}_4$  phosphors were  $x = 0.6687$  and  $y = 0.3311$ . Figure 7 illustrates the CIE chromaticity diagram for the emissions of pure and  $\text{Sm}^{3+}$ , (1.0 mol %) doped  $\text{Sr}_2\text{CeO}_4$ . This phosphor having colour tenability from blue to white light and has potential for application in the lighting system.

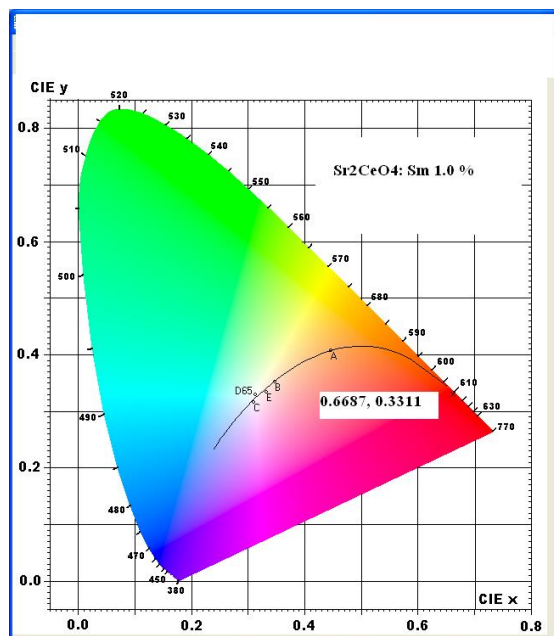


Figure 7: CIE co-ordinates for  $\text{Sr}_2\text{CeO}_4: \text{Sm}^{3+}$

### CONCLUSION

$\text{Sr}_2\text{CeO}_4: x\text{Sm}^{3+}$  ( $x = 0.5, 1.0, 2\%$ ), was successfully synthesized by solid state reaction method. The XRD study confirms that the  $\text{Sm}^{3+}$  doped  $\text{Sr}_2\text{CeO}_4$  compound has orthorhombic structure at room temperature. The EDS studies confirm the formation of  $\text{Sr}_2\text{CeO}_4: \text{Sm}^{3+}$ . The average crystallite size of the trivalent Samarium doped with  $\text{Sr}_2\text{CeO}_4$  the crystallite size is 68 nm. The emission peaks at 568nm corresponds to  ${}^4\text{G}_{5/2} \rightarrow {}^6\text{H}_{5/2}$ , 611nm corresponds to  ${}^4\text{G}_{5/2} \rightarrow {}^6\text{H}_{7/2}$  and the transition 653nm corresponds to  ${}^4\text{G}_{5/2} \rightarrow {}^6\text{H}_{9/2}$ , the strongest emission peak located at 611 nm showing prominent and red light is due to the  ${}^4\text{G}_{5/2} \rightarrow {}^6\text{H}_{7/2}$  transition of  $\text{Sm}^{3+}$ . The color co-ordinates for  $\text{Sr}_2\text{CeO}_4: 1.0 \text{ mol } \%$   $\text{Sm}^{3+}$  were  $x = 0.6687$  and  $y = 0.3311$ . Solid state reaction method proved to be very promising for the controlled preparation of phosphor material, with an even better CIE chromacity index than reported previously. The result shows this phosphor has potential application in the field of emission devices.

### ACKNOWLEDGMENTS

The author expresses their sincere thanks to Prof. K.V.R. Murthy to provide lab facility. Also thankful to Dr. N. O. Girase, the Principal, and Dr. K. D. Girase, vice Principal, S. V. S's Dadasaheb Rawal College Dondaicha for continuous encouragement.

### REFERENCES

1. S Shionoya, W Yen, H Yamamoto. Phosphor Handbook, CRC Press, Boca Raton, FL (USA), 2007.
2. Liqiong An, Jian Zhang, Min Liu, Shi Chen, Shiwei Wang. Preparation and photoluminescence of  $\text{Sm}^{3+}$  and  $\text{Eu}^{3+}$  doped  $\text{Lu}_2\text{O}_3$  phosphor. Optical Mat. 2008; 30; 957-960.
3. Fu Shi-Liu; Yin Tao; Chi Fei. Synthesis and characterization of  $\text{Ca}_2\text{Sn}_{1-x}\text{Ce}_x\text{O}_4$  with blue luminescence originating from  $\text{Ce}^{4+}$  charge transfer transition. Chinese Physics. 2007; 16 (10); 3129-3133.
4. Danielson E, Devenney M, Giaquinta DM, Golden JH, Haushalter RC, McFarland EW, et al. A Rare-Earth Phosphor Containing One-Dimensional Chains Identified Through Combinatorial Methods. Science. 1998; 279; 837-839.
5. Chunxiang Zhang, Wenjun Jiang, Xujie Yang, Qiaofeng Han, Qingli Hao, Xin Wang. Synthesis and luminescent property of  $\text{Sr}_2\text{CeO}_4$  phosphor via EDTA-complexing process] Alloys and Compounds. 2009; 474(1-2); 287-291,
6. Zhang Chunxiang; Shi Jianshe; Yang Xujie; Lu Lude; Wang Xin. Preparation, characterization and luminescence of  $\text{Sm}^{3+}$  or  $\text{Eu}^{3+}$ -doped  $\text{Sr}_2\text{CeO}_4$  by a modified sol-gel method. J Rare earths. 2010; 28(4); 513- 518.
7. Pradip Z Zambare, AP Zambare, KVR Murthy, OH Mahajan. Synthesis and Characterization of Red Emitting  $\text{Sr}_2\text{CeO}_4: \text{Eu}^{3+}$  Nano Phosphors. J Chem Pharm Res. 2012;4(4);1990-1994.
8. T Masui, T Chiga, N Imanaka, G.-Y Adachi. Synthesis and luminescence of  $\text{Sr}_2\text{CeO}_4$  fine particles. Mater Res Bull. 2003;38(1):17- 24.
9. Haiyan JIAO, Yuhuab WANG, Jiachi Zhang. Journal of Physics: Conference Series 2009; 152; 012089.
10. Chang-Hsin Lu, Chang-Tao Chen. Luminescent characteristics and microstructures of  $\text{Sr}_2\text{CeO}_4$  phosphors prepared via sol-gel and solid-state reaction routes] sol-gel sci. Technol. 2007; 43(2); 179-185.
11. Niyaz Parvin Shaik, NV Poornchandra Rao, B Subba Rao, KVR Murthy. Photoluminescence Studies on  $\text{Sr}_2\text{CeO}_4$  Nanophosphor World J Chem. 2011; 6(2); 115-117.

12. Roshani Singh, SJ Dhoble.  $\text{Eu}^{3+}$  and  $\text{Dy}^{3+}$  activated  $\text{Sr}_2\text{V}_2\text{O}_7$  phosphor for solid state lighting. Adv Mat Lett. 2011;2(5);341–344.
13. Color Calculator version 2, software from Radiant Imaging, Inc, 2007,
14. KN Shinde, SJ Dhoble. Influence of  $\text{Li}^+$  doping on photoluminescence properties of  $\text{Sr}_5(\text{PO}_4)_3\text{F}:\text{Eu}^{3+}$ . Adv Mat Lett. 2010; 1(3); 254–258.
15. George Blasse, BC Grabmaier Luminescent Materials, Springer–Verlag, 1994